Analysis of Truss Structures with Uncertainties: From Experimental Data to Analytical Responses

P. Longo[1)], N. Maugeri[1)], G. Muscolino[2)] and G. Ricciardi[2)]
[1)] Department of Engineering, University of Messina, Villaggio S. Agata, 98166 Messina, Italy, {plongo, nmaugeri}@unime.it

[2)] Department of Engineering and Inter-University Centre of Theoretical and Experimental Dynamics, University of Messina, Villaggio S. Agata, 98166 Messina, Italy, {gmuscolino, gricciardi}@unime.it

Abstract: This paper deals with the analysis of truss structures with uncertain elastic modulus under deterministic loads. The uncertain parameters, which characterize the elastic modulus, are determined by examining the experimental data obtained from tensile tests on several steel bars performed in the Laboratory of Structures and Materials of the Department of Engineering (University of Messina). Analyzing the experimental data, both the probabilistic and non-probabilistic models are examined. In the first case the random uncertainties are completely characterized through the knowledge of the probability density function, which is determined by applying the maximum entropy approach and compared with Gaussian model. In the second case the interval model is adopted and the uncertainties are characterized by the midpoint and deviation values. Finally, in order to compare the propagation of these two models of uncertainties, the response of a benchmark truss structure is evaluated and the results in terms of displacements are compared.

Keywords: probabilistic uncertainties, maximum entropy approach, interval analysis, rational series expansion

1. Introduction

In recent years it has been recognized that the analysis of structural systems should take into account all the relevant uncertainties present in the analyzed problem. Uncertainties associated with an engineering problem, due to the different sources, can be divided into two main groups: *random uncertainties* and *epistemic uncertainties* (Elishakoff and Ohsaki, 2010). The random uncertainties are completely characterized through the knowledge of the full set of its statistics (which could be moments, cumulants or other derived quantities) or, which is the same, through the knowledge of its *probability density function* (*PDF*). Despite their success, unfortunately the probabilistic approaches give reliable results only when sufficient experimental data are available to define the *PDF* of the fluctuating properties. If available information are fragmentary or incomplete so that only bounds on the magnitude of the uncertain structural parameters are known, non-probabilistic approaches can be alternatively applied. In the framework of non-probabilistic approaches the interval model, which stems from *interval analysis* (see e.g. Moore, 1966; Moore et al., 2009), may be considered as the most widely used analytical tool among non-probabilistic methods (Muhanna and Mullen, 2001; Moens and Vandepitte, 2005). According to this approach, the fluctuating structural parameters are treated as interval numbers inside their lower and upper bounds.

In the framework of probabilistic approaches usually the uncertainties are assumed as stochastic variables modelled by Gaussian distributions. However, often, this distribution does not reflect the actual one. As a consequence the numerical results obtained by assuming the Gaussian approximations could be very far from the effective ones. On the contrary in this paper, starting from data obtained from experiments on several steel bars performed in the Laboratory of Structures and Materials of the Department of Engineering (University of Messina), the *PDF* of elastic modulus of the material is derived by applying the maximum entropy approach proposed by Alibrandi and Ricciardi (2008). Then the probabilistic response of a benchmark truss structures is determined once the inverse of the global stochastic stiffness matrix is evaluated in approximate explicit closed form by applying the recently proposed *Rational Series Expansion* (*RSE*) (Muscolino and Sofi, 2013; Muscolino et al., 2014). So operating a substantial computational savings over classical Monte Carlo Simulation (*MCS*) is obtained.

In the framework of interval analysis the midpoint and deviation values of the uncertain elastic modulus are determined by analyzing experimental data. Then, approximate explicit expressions of the bounds of the interval nodal displacements of the benchmark truss structures are derived by applying the so-called *Interval Rational Series Expansion* (*IRSE*) (Muscolino and Sofi, 2013; Muscolino et al., 2014) recently proposed to evaluate the explicit inverse of the global stiffness matrix with interval modifications.

2. Preliminary concepts and definitions

2.1. Equations Governing the Problem of Truss Structures

It is well known that the equilibrium equations of a truss structure with n unconstrained nodal displacements and m elements, subjected to known static loads, can be written as follows:

$$\begin{aligned} &\mathbf{C}^T\mathbf{Q} = \mathbf{f}\,; &&\text{equilibrium equation;}\\ &\mathbf{Q} = \mathbf{R}\,\mathbf{q}\,; &&\text{constitutive equation;}\\ &\mathbf{C}\,\mathbf{U} = \mathbf{q}. &&\text{compatibility equation.}\end{aligned} \tag{1a,b,c}$$

where $\mathbf{U}$ is the is the vector, of order n, of nodal displacements; $\mathbf{f}$ is the vector, of order n, collecting the external loads applied at the nodes; $\mathbf{Q}$ and $\mathbf{q}$ are the vectors , of order m, of internal forces and deformations respectively; $\mathbf{C}^T$ is the $n \times m$ equilibrium matrix and $\mathbf{R}$ is the $m \times m$ diagonal internal stiffness matrix. Let us now indicate with $\rho_j = E_j A_j / L_j$ the axial stiffness of the j-th element, where E_j, A_j and L_j are the Young elastic modulus, the area and the length of the j-th element, respectively. Let us assume now that $r \le m$ elements possess uncertain elastic modulus. Denoting with α_j the dimensionless fluctuation of the j-th uncertain elastic modulus around the nominal value, $E_{0,j}$, of the j-th element, such that $E_j = E_{0,j}\left(1+\alpha_j\right)$, one gets:

$$\rho_j = E_{0,j}\left(1+\alpha_j\right)A_j \big/ L_j = \rho_{0,j}(1+\alpha_j) \tag{2}$$

where $\rho_{0,j} = E_{0,j}\,A_j \big/ L_j$ is the nominal value of the axial stiffness of the *j*-thelement with $j = 1,2,\ldots,r \le m$. Then, the internal stiffness matrix $\mathbf{R}(\boldsymbol{\alpha})$ can be written as:

$$\mathbf{R}(\boldsymbol{\alpha}) = \mathbf{R}_0 + \sum_{j=1}^{r} \alpha_j\, \mathbf{l}_{E,j}\mathbf{l}_{E,j}^T, \tag{3}$$

where $\boldsymbol{\alpha}$ is the vector collecting the *r* uncertain dimensionless fluctuations α_j, $\mathbf{R}_0$ is the diagonal nominal internal stiffness matrix and $\mathbf{l}_{E,j}$ is a vector of order *n* with only the *j*-th element equal to $\sqrt{\rho_{0,j}}$ and the other ones equal to zero. Notice that the dyadic product $\mathbf{l}_{E,j}\mathbf{l}_{E,j}^T$ gives a change of rank one to the nominal internal stiffness matrix. After simple substitutions into Eqs. (1) the solving equilibrium equation, in the framework of the displacement method, can be written as:

$$\mathbf{K}(\boldsymbol{\alpha})\mathbf{U}(\boldsymbol{\alpha}) = \mathbf{f} \tag{4}$$

where $\mathbf{U}(\boldsymbol{\alpha})$ is the vector, of order n, of the unknown nodal displacement depending on uncertainties and $\mathbf{K}(\boldsymbol{\alpha})$ is the uncertain stiffness matrix which, by means of Eqs. (1), can be written as:

$$\mathbf{K}(\boldsymbol{\alpha}) = \mathbf{C}^T\mathbf{R}(\boldsymbol{\alpha})\ \mathbf{C} \tag{5}$$

Then, according to Eq. (3), the stiffness matrix $\mathbf{K}(\boldsymbol{\alpha})$, which possesses r uncertain parameters. can be rewritten as:

$$\mathbf{K}(\boldsymbol{\alpha}) = \mathbf{K}_0 + \sum_{j=1}^{r} \alpha_j\, \mathbf{K}_j\ = \mathbf{K}_0 + \Delta\mathbf{K}\left(\boldsymbol{\alpha}\right) \tag{6}$$

where $\mathbf{K}_0$ is the nominal stiffness matrix and $\mathbf{K}_j$ is a rank-one matrix defined respectively as:

$$\mathbf{K}_0 = \mathbf{C}^T\ \mathbf{R}_0\ \mathbf{C}\,;\quad \mathbf{K}_j = \mathbf{v}_j\ \mathbf{v}_j^T \tag{7a,b}$$

with the vector $\mathbf{v}_j$ given as:

$$\mathbf{v}_j = \mathbf{C}^T\ \mathbf{l}_{E,j} \tag{8}$$

Finally, the solution of Eq. (4) can be formally written as:

$$\mathbf{U}(\boldsymbol{\alpha}) = \mathbf{K}(\boldsymbol{\alpha})^{-1}\,\mathbf{f} \tag{9}$$

Because of the presence in Eq. (9) of the vector $\boldsymbol{\alpha}$, collecting the uncertain dimensionless fluctuations α_j, the solution of previous equation can be obtained efficiently if explicit expressions of the inverse of the random stiffness matrix $\mathbf{K}(\boldsymbol{\alpha})$ are known. To do this, in the next subsection a new series expansion is described.

2.2. EXPLICIT INVERSE OF THE STIFFNESS MATRIX FOR STRUCTURAL SYSTEM WITH RANK-ONE MODIFICATIONS

In order to derive the explicit expression of the inverse of the stiffness matrix, in this section a recently proposed series expansion, called *Rational Series Expansion* (*RSE*), is described (Muscolino and Sofi, 2013; Muscolino et al., 2014). The *RSE* has been obtained by properly modifying the Neumann series expansion in the case of structural systems with more rank-one modifications in the stiffness matrix. So operating an approximate explicit expression of the inverse of an invertible matrix with r modifications was derived. In particular, for truss structures, the matrix $\Delta\mathbf{K}(\boldsymbol{\alpha})$, which collects the rank-r change in the stiffness matrix, can be written as the superposition of r rank-one matrices as follows:

$$\Delta\mathbf{K}(\boldsymbol{\alpha}) = \sum_{i=1}^{r} \alpha_i \mathbf{v}_i \ \mathbf{v}_i^T \tag{10}$$

where the vector $\mathbf{v}_i$ has been defined in Eq. (8). Moreover, since the fluctuating dimensionless uncertainties are lesser than one, that is $|\alpha_s| \ll 1$, it is possible to evaluate in explicit form the approximate inverse of stiffness matrix by retaining only the first order term as follows:

$$\mathbf{K}(\boldsymbol{\alpha})^{-1} = \left[\mathbf{K}_0 + \sum_{i=1}^{r} \alpha_i \mathbf{v}_i \ \mathbf{v}_i^T\right]^{-1} \approx \mathbf{K}_0^{-1} - \sum_{i=1}^{r} \frac{\alpha_i}{1+\alpha_i d_i} \mathbf{D}_i \tag{11}$$

where the following quantities have been introduced:

$$d_i = \mathbf{v}_i^T \mathbf{K}_0^{-1} \mathbf{v}_i; \quad \mathbf{D}_i = \mathbf{K}_0^{-1} \mathbf{v}_i \ \mathbf{v}_i^T \mathbf{K}_0^{-1}. \tag{12a,b}$$

Notice that Eq. (11) certainly holds if the following condition is satisfied:

$$|\alpha_i \, d_i| < 1. \tag{13}$$

2.3. EXPLICIT MEAN-VALUE VECTOR AND COVARIANCE MATRIX FOR STOCHASTIC UNCERTAINTIES

This section addresses the problem of static analysis of structures in which the uncertainties are modelled as zero-mean stochastic independent variables $\tilde{\alpha}_i$, with assigned *Probability Density Function* (*PDF*) $p_{\tilde{\alpha}_i}(x)$, collected in the vector $\tilde{\boldsymbol{\alpha}}$. In this case the solution of equilibrium equations depend on stochastic variables, that is:

$$\mathbf{K}(\tilde{\boldsymbol{\alpha}})\,\mathbf{U}(\tilde{\boldsymbol{\alpha}}) = \mathbf{f} \tag{14}$$

where the tilde denotes a stochastic quantity. By applying Eq. (11), the inverse of the stochastic matrix $\mathbf{K}(\tilde{\boldsymbol{\alpha}})$ can be evaluated as:

$$\mathbf{K}(\tilde{\boldsymbol{\alpha}})^{-1} = \left[\mathbf{K}_0 + \sum_{i=1}^{r} \tilde{\alpha}_i \mathbf{v}_i \ \mathbf{v}_i^T\right]^{-1} \approx \mathbf{K}_0^{-1} - \sum_{i=1}^{r} \frac{\tilde{\alpha}_i}{1+\tilde{\alpha}_i d_i} \mathbf{D}_i \tag{15}$$

where $\mathbf{K}_0$ is the stiffness matrix of the nominal system while d_i and $\mathbf{D}_i$ have been defined in Eq. (12).

Accordingly, the solution of the set of linear stochastic Eq. (14) can be written in the following approximate explicit form:

$$\mathbf{U}(\tilde{\boldsymbol{\alpha}}) \equiv \tilde{\mathbf{U}} = \mathbf{K}(\tilde{\boldsymbol{\alpha}})^{-1}\mathbf{f} \approx \mathbf{K}_0^{-1}\mathbf{f} - \sum_{i=1}^{r} \frac{\tilde{\alpha}_i}{1+\tilde{\alpha}_i d_i}\mathbf{D}_i\,\mathbf{f} \tag{16}$$

Finally, since zero-mean stochastic variables $\tilde{\alpha}_i$ are realistically assumed independent ones, the mean-value vector and the covariance matrix of the stochastic response vector $\tilde{\mathbf{U}}$ can be evaluated, respectively, as follows:

$$\begin{aligned}
\boldsymbol{\mu}_{\tilde{\mathbf{U}}} &= \mathrm{E}\langle \tilde{\mathbf{U}} \rangle \approx \mathbf{K}_0^{-1}\mathbf{f} - \sum_{i=1}^{r} \mathrm{E}\left\langle \frac{\tilde{\alpha}_i}{1+\tilde{\alpha}_i d_i} \right\rangle \mathbf{D}_i\,\mathbf{f};\\
\boldsymbol{\Sigma}_{\tilde{\mathbf{U}}} &= \mathrm{E}\langle \tilde{\mathbf{U}}\tilde{\mathbf{U}}^T \rangle - \boldsymbol{\mu}_{\tilde{\mathbf{U}}}\boldsymbol{\mu}_{\tilde{\mathbf{U}}}^T \approx \sum_{i=1}^{r}\left[\mathrm{E}\left\langle \left(\frac{\tilde{\alpha}_i}{1+\tilde{\alpha}_i d_i}\right)^2 \right\rangle - \left(\mathrm{E}\left\langle \frac{\tilde{\alpha}_i}{1+\tilde{\alpha}_i d_i} \right\rangle \right)^2 \right] \mathbf{D}_i\,\mathbf{f}\,\mathbf{f}^T\mathbf{D}_i
\end{aligned} \tag{17a,b}$$

where $\mathrm{E}\langle \bullet \rangle$ is the stochastic operator defined as:

$$\mathrm{E}\left\langle \frac{\tilde{\alpha}_i}{1+\tilde{\alpha}_i d_i} \right\rangle = \int_{-\infty}^{\infty}\left[\frac{x}{1+x\,d_i}\right] p_{\tilde{\alpha}_i}(x)\,\mathrm{d}x; \quad \mathrm{E}\left\langle \left(\frac{\tilde{\alpha}_i}{1+\tilde{\alpha}_i d_i}\right)^2 \right\rangle = \int_{-\infty}^{\infty}\left[\frac{x}{1+x\,d_i}\right]^2 p_{\tilde{\alpha}_i}(x)\,\mathrm{d}x. \tag{18a,b}$$

Obviously, if the stochastic variable is defined in a finite interval $[a,b]$ the previous relationships can be rewritten as:

$$\mathrm{E}\left\langle \frac{\tilde{\alpha}_i}{1+\tilde{\alpha}_i d_i} \right\rangle = \int_{a}^{b}\left[\frac{x}{1+x\,d_i}\right] p_{\tilde{\alpha}_i}(x)\,\mathrm{d}x; \quad \mathrm{E}\left\langle \frac{\tilde{\alpha}_i}{1+\tilde{\alpha}_i d_i} \right\rangle^2 = \int_{a}^{b}\left[\frac{x}{1+x\,d_i}\right]^2 p_{\tilde{\alpha}_i}(x)\,\mathrm{d}x. \tag{19a,b}$$

The previous equations provide substantial computational savings over classical MCS method since they just involve the statistics of the random variables $\tilde{\alpha}_i \,/\,(1+\tilde{\alpha}_i d_i)$ without requiring the inversion of the global stochastic stiffness matrix. Furthermore, the closed-form expression of the random response in Eq. (16) enables one to evaluate higher-order statistical moments useful to determine the *PDF* of the response.

2.4. Explicit Bounds of the Response for Interval Uncertainties

Let us consider now the case in which the uncertainties are modelled with uncertain-but-bounded parameters modeled as interval variables. According to interval analysis, the vector $\boldsymbol{\alpha}$, of order *r*, in this case has to be defined as: $\boldsymbol{\alpha}^I = [\underline{\boldsymbol{\alpha}}, \overline{\boldsymbol{\alpha}}]$. In the following with the apex *I* is denoted an interval quantity. The vector $\boldsymbol{\alpha}^I$, collects the *r* uncertain-but-bounded symmetric fluctuations of axial stiffness around their nominal value and defines a *r*-dimension bounded convex set-interval vector of real numbers, such that

$\underline{\boldsymbol{\alpha}} \leq \boldsymbol{\alpha} \leq \overline{\boldsymbol{\alpha}}$ whose *i*-th element is α_i^I. Without loss of generality it is assumed the midpoint value vector, $\boldsymbol{\alpha}_0$, equals to **0**. Then the deviation amplitude vector, $\Delta\boldsymbol{\alpha}$, which collect the fluctuations around the midpoint is given as:

$$\boldsymbol{\alpha}_0 = \mathbf{0} \quad \Rightarrow \quad \Delta\boldsymbol{\alpha} = \frac{1}{2}\left(\overline{\boldsymbol{\alpha}} - \underline{\boldsymbol{\alpha}}\right) = \overline{\boldsymbol{\alpha}} = -\underline{\boldsymbol{\alpha}} \tag{20a,b}$$

where the symbols $\underline{\boldsymbol{\alpha}}$ and $\overline{\boldsymbol{\alpha}}$ denote the lower and upper bound vectors respectively. As a consequence of Eqs. (20), the following relationship holds for the generic interval variable

$$\alpha_i^I = \Delta\alpha_i \, \hat{e}_i^I \tag{21}$$

where $\hat{e}_i^I \triangleq [-1,+1] \quad (i = 1,2,\cdots,r)$ is the so-called *Extra Unitary Interval* (*EUI*) (Muscolino and Sofi, 2012; Muscolino and Sofi, 2013).

For deterministic static loads and uncertain-but-bounded parameters, the equilibrium Eq. (5) can be rewritten as:

$$\mathbf{K}(\boldsymbol{\alpha}^I)\,\mathbf{u}(\boldsymbol{\alpha}^I) = \mathbf{f} \tag{22}$$

It follows that the stiffness matrix $\mathbf{K}(\boldsymbol{\alpha}^I)$, depends only on deviation amplitude value of the *r* uncertain-but-bounded parameters and according to interval formalism is written as:

$$\mathbf{K}\left(\boldsymbol{\alpha}^I\right) = \mathbf{K}_0 + \sum_{i=1}^{r} \Delta\alpha_i \hat{e}_i^I \mathbf{v}_i \mathbf{v}_i^T = \mathbf{K}_0 + \sum_{i=1}^{r} \hat{e}_i^I \Delta\mathbf{K}_i \tag{23}$$

where:

$$\Delta\mathbf{K}_i = \Delta\alpha_i \mathbf{v}_i \mathbf{v}_i^T \tag{24}$$

The goal is now to find the narrowest interval $\mathbf{u}^I$ containing all possible response vectors $\mathbf{u}$, satisfying the equilibrium Eq. (22), when the vector $\boldsymbol{\alpha}$ assumes all possible values inside the interval vector $\boldsymbol{\alpha}^I$. The problem is formally solved as:

$$\mathbf{u}^I = \left(\mathbf{K}\left(\boldsymbol{\alpha}^I\right)\right)^{-1} \mathbf{f} \tag{25}$$

Since in structural engineering the stiffness matrix is regular and it can be assumed that the uncertainties are not large, so that $\Delta\alpha_i \ll 1 \; \forall i$, the inverse interval of the stiffness matrix, by applying the *Improved Interval Analysis* (Muscolino and Sofi, 2012), can be determined by the applying so called *Interval Rational Series Expansion* (*IRSE*) (Muscolino and Sofi, 2013; Muscolino and al., 2014) as (see Eq. (11)):

$$\mathbf{K}\left(\boldsymbol{\alpha}^I\right)^{-1} = \left(\mathbf{K}_0 + \sum_{i=1}^{r} \Delta\alpha_i \, \hat{e}_i^I \mathbf{v}_i \; \mathbf{v}_i^T\right)^{-1} \approx \mathbf{K}_0^{-1} - \sum_{i=1}^{r} \frac{\Delta\alpha_i \, \hat{e}_i^I}{1 + \Delta\alpha_i \, \hat{e}_i^I d_i} \mathbf{D}_i \tag{26}$$

Obviously, the accuracy of Eq. (26), which gives the explicit inverse of a matrix with r fluctuating parameters, depends on the magnitude of the fluctuations $\Delta\alpha_i$. Alternatively, Eq. (26) can be rewritten in the so-called affine form (Muscolino and Sofi, 2013) as:

$$\mathbf{K}\left(\boldsymbol{\alpha}^I\right)^{-1}=\left(\mathbf{K}_0+\sum_{i=1}^{r}\Delta\alpha_i\,\hat{e}_i^I\mathbf{v}_i\,\mathbf{v}_i^T\right)^{-1}\approx\mathbf{K}_0^{-1}+\sum_{i=1}^{r}\left(a_{0,i}+\Delta a_i\,\hat{e}_i^I\right)\mathbf{D}_i \tag{27}$$

where $a_{0,i}$ and Δa_i are given by:

$$a_{0,i}=\frac{\left(\Delta\alpha_i\right)^2 d_i}{1-\left(\Delta\alpha_i\,d_i\right)^2}>0;\quad \Delta a_i=\frac{\Delta\alpha_i}{1-\left(\Delta\alpha_i\,d_i\right)^2}>0. \tag{28a,b}$$

Then the solution of Eq. (22) is given respectively as:

$$\mathbf{u}^I=\mathbf{K}\left(\boldsymbol{\alpha}^I\right)^{-1}\mathbf{f}\approx\mathbf{K}_0^{-1}\mathbf{f}+\sum_{i=1}^{r}\left(a_{0,i}+\Delta a_i\,\hat{e}_i^I\right)\mathbf{D}_i\mathbf{f} \tag{29}$$

Due to the monotonicity of the components of the vector $\mathbf{u}(\boldsymbol{\alpha}^I)$ with respect to the generic $\Delta\alpha_i$, the lower and upper bounds of displacements can be evaluated respectively as:

$$\underline{\mathbf{u}}=\mathbf{u}_0-\Delta\mathbf{u};\quad \overline{\mathbf{u}}=\mathbf{u}_0+\Delta\mathbf{u} \tag{30a,b}$$

where the following vectors are introduced:

$$\mathbf{u}_0=\mathbf{K}_0^{-1}\mathbf{f}+\sum_{i=1}^{r}a_{0,i}\,\mathbf{D}_i\,\mathbf{f};\quad \Delta\mathbf{u}=\sum_{i=1}^{r}\Delta a_i\left|\mathbf{D}_i\,\mathbf{f}\right| \tag{31a,b}$$

with the symbol $|\bullet|$ which denotes the *component wise* absolute value.

3. Probability density function derived by experimental data

In the framework of structural engineering usually the uncertainties are assumed as stochastic variables modelled by Gaussian distributions. However, often, this distribution does not reflect the actual one. As a consequence the numerical results obtained by assuming the Gaussian approximations could be very far from the effective ones. To overcome this drawback, in this section, a method to derive the distribution coherent in some way with the histogram obtained analysing the results of a set of experimental data is presented. The method is based on the maximum entropy principle proposed by Alibrandi and Ricciardi (2008), which derived the effective *PDF* coherent with experimental data in terms of moments.

Let denote with $\hat{p}_{\tilde{X}}(x)$ the approximating *PDF* of the given random variable $\tilde{X}$, defined in a finite interval $[a,b]$, which can be written as superposition of basis *PDF* $\varphi_{\tilde{X}}^{(i)}(x;x_i,h_i)$:

$$\hat{p}_{\tilde{X}}(x)=\sum_{i=1}^{N}p_i\,\varphi_{\tilde{X}}^{(i)}(x;x_i,h_i) \tag{32}$$

where the i-th basis *PDF* $\varphi_{\tilde{X}}^{(i)}\left(x;x_i,h_i\right)$, having unitary area in the interval domain $[a,b]$, depends on the location x_i and bandwidth h_i. The location parameters are N points belonging to the domain $[a,b]$, chosen for sake of simplicity with a constant step $\Delta x = x_{i+1} - x_i$, (with $i = 1,2,\ldots,N-1$). In a similar way it has been assumed a constant bandwidth parameter $h_i = h = q\,\Delta x$, a good choice is $q = 2/3$.

The superposition of basis *PDF* (Eq. (32)) represents a *PDF* if and only if the coefficients p_i satisfy the following conditions:

$$\begin{cases} 0 \le p_i < 1, \qquad i = 1\ldots N \\ \sum_{i=1}^{N} p_i = 1 \end{cases} \tag{33}$$

Equations (32) and (33) show that a generic *PDF* can be expressed as a linear convex combination of simpler *PDF*s, whose coefficients have the meaning of probabilities. In order to evaluate the probabilities p_i, it is useful to rewrite Eq. (32) as follows:

$$\hat{p}_{\tilde{X}}\left(x\right) = \boldsymbol{\varphi}_{\tilde{X}}^{T}\left(x\right)\mathbf{p} \tag{34}$$

where $\boldsymbol{\varphi}_{\tilde{X}}^{T}\left(x\right) = \left[\varphi_{\tilde{X}}^{(1)}\left(x;x_1,h\right),\varphi_{\tilde{X}}^{(2)}\left(x;x_2,h\right),\cdots,\varphi_{\tilde{X}}^{(N)}\left(x;x_N,h\right)\right]$ and $\mathbf{p}^T = \left[p_1,p_2,\cdots,p_N\right]$ are vectors of order N. Multiplying both sides of Eq. (34) by x^k (with $k = 0,1,2,\ldots,M$). and integrating over the domain, taking into account Eqs. (33), the following system of equations is obtained:

$$\begin{cases} \mathbf{1}^{\mathbf{T}}\mathbf{p} = 1 \\ \mathbf{M}\,\mathbf{p} = \boldsymbol{\mu} \end{cases} \tag{35a,b}$$

where **1** is a unit vector of order N, $\mathbf{M}$ is a matrix of order $M \times N$, whose elements, m_{ki}, are the moments of order k of the i-th basis *PDF* $\varphi_{\tilde{X}}^{(i)}\left(x;x_i,h_i\right)$:

$$m_{ki} = \int_a^b x^k\ \varphi_{\tilde{X}}^{(i)}\left(x;x_i,h_i\right)\mathrm{d}x \tag{36}$$

while $\boldsymbol{\mu}$ is a vector of order M collecting the k-th moment derived from experimental data. In the system of equations (Eq. (35)) the number of moments M gives the data information. Here it is assumed that only the lower six moments ($M \le 6$) can be derived with good accuracy from experimental data.

The number N of kernel densities gives the resolution for the recovery of the target *PDF* $p_{\tilde{X}}\left(x\right)$; as much as N increases, computational complexity grows; it’s a good choice to select N in the range 20-100, being generally N lower than the N_s sample data.

To solve the system (Eq. (35)) the Maximum Entropy method is adopted, that leads to find the unique minimum of the free functional $H^{ME} = H\left(\lambda_1,\lambda_2,\ldots,\lambda_M\right)$, where λ_i is the i-th Lagrange multiplier, defined as (Alibrandi and Ricciardi, 2008):

$$H^{ME} = H\left(\lambda_1, \lambda_2, \ldots, \lambda_M\right) = \lambda_0 + \sum_{k=1}^{M} \lambda_k \cdot \mu_k \tag{37}$$

where

$$\lambda_0 = \lambda_0\left(\lambda_1, \lambda_2, \ldots, \lambda_M\right) = \ln\left[\sum_{i=1}^{N} \exp\left(-\sum_{k=1}^{M} \lambda_k \cdot x_i^k\right)\right] \tag{38}$$

is the normalization constant, that can be expressed as a function of $\lambda_1, \lambda_2, ., \lambda_M$, and

$$\mu_k = \mu_k\left(\lambda_1, \lambda_2, \ldots, \lambda_M\right) = \frac{\sum_{i=1}^{N} x_i^k \cdot \exp\left(-\sum_{j=1}^{M} \lambda_j x_i^k\right)}{\sum_{i=1}^{N} \exp\left(-\sum_{j=1}^{M} \lambda_j x_i^k\right)} \tag{39}$$

The free function $H^{ME} = H\left(\lambda_1, \lambda_2, \ldots, \lambda_M\right)$ is convex with respect to the Lagrange multipliers $\lambda_1, \lambda_2, \ldots, \lambda_M$ and, as a consequence, it has an unique minimum , which can be obtained through a standard convex optimization algorithm, with a limited number of iterations.

The corresponding coefficients p_i can be computed as:

$$p_i = \exp\left(-\lambda_0 - \sum_{k=1}^{M} \lambda_k \cdot x_i^k\right) \tag{40}$$

where the Lagrange multipliers are solution of the Maximum Entropy optimization problem (Alibrandi and Ricciardi, 2008).

4. Numerical results versus experimental data

Aim of this study is to perform the analysis of truss structures with uncertain Young elastic modulus under deterministic loads by applying both probabilistic and non-probabilistic approaches. To do this the Young elastic modulus is determined by several experiments on steel bars performed in the Laboratory of Structures and Materials of the Department of Engineering (University of Messina). Tensile strength tests, according to UNI EN ISO 15630-1, were performed on 128 specimens, using universal machine, Galdabini VB47, Quasar 1200 and elastic modulus was computed by electronic extensometer micron motor (class 0.5 according to UNI EN ISO 9513). The main statistics of experimental data: *Coefficient of Variation* (*CoV*), $\mu_{\tilde{\alpha}} / \sigma_{\tilde{\alpha}}$; *skewness coefficient*, $\mu_{3,\tilde{\alpha}} / \sigma_{\tilde{\alpha}}^3$, and *excess kurtosis*, $(\mu_{4,\tilde{\alpha}} / \sigma_{\tilde{\alpha}}^4) - 3$, are reported in Table I.

In this section, the described procedure is applied to the benchmark truss structure depicted in Figure 1. The cross-sectional areas and Young's moduli of five bars are A_1=A_2=A_3=A_4=A_5=0.0009 [m^2] and $E_{0,1}$=$E_{0,2}$=$E_{0,3}$=$E_{0,4}$=$E_{0,5}$=2.1 10^6 [N/mm^2] respectively. In particular, first, in the framework of probabilistic approaches, the statistics of the response are evaluated by applying the proposed formulation and compared with the same obtained by *Monte Carlo Simulation* (*MCS*). Then, by applying the *Improved Interval Analysis*, the bounds of nodal response in terms of displacements are evaluated.

Table I. Statistical results for Young Elastic Modulus from experimental data.

N. Samples	128
Mean: $\mu_{\tilde{\alpha}}$ [N/mm^2]	198110.68
Standard Deviation: $\sigma_{\tilde{\alpha}}$ [N/mm^2]	13868.14
Minimum [N/mm^2]	161742.41
Median [N/mm^2]	198147.39
Maximum [N/mm^2]	240816.20
CoV	0.07
Skewness Coefficient	0.4188
Excess Kurtosis	4.8246

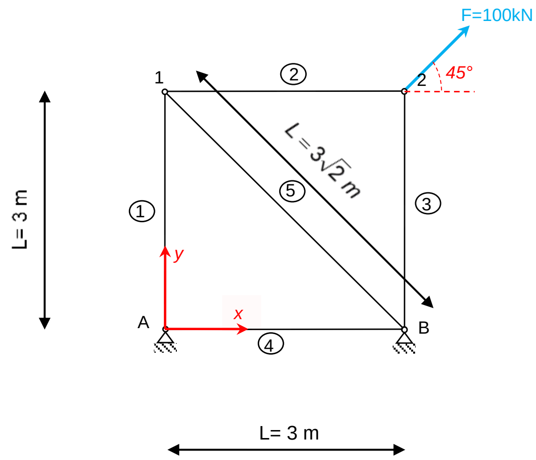

Figure 1. Sketch of benchmark truss system.

4.1. PROBABILISTIC APPROACH

In the framework of the probabilistic approach and according to the Chauvenet criterion for the selection of the effective experimental results (Barbato et al., 2011), the *Kernel PDF* of the Young elastic modulus is evaluated in the interval domain [*a*,*b*] of existence of *PDF* which is chosen as $\left[\mu_{\tilde{\alpha}} - 4.0\sigma_{\tilde{\alpha}}, \mu_{\tilde{\alpha}} + 4.0\sigma_{\tilde{\alpha}}\right]$; then, to avoid numeric instability, the interval is normalized into the domain [0,1]. Finally the *Kernel PDF* is determined, according to Eq. (32), as a linear combination of 30 normal basis kernel densities, whose coefficient p_i are computed by Eq. (40) once the Maximum Entropy optimization problem is solved (Alibrandi and Ricciardi, 2008).

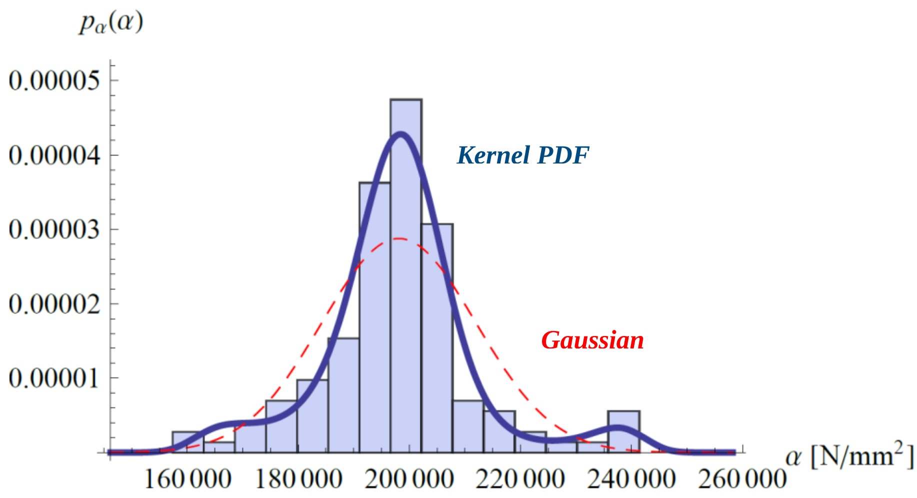

Figure 2. Comparison between *Kernel PDF*, *Gaussian PDF* and experimental data.

The *Kernel PDF* is depicted in Figure 2 together with the histogram of experimental data and the *Gaussian PDF* having same mean value and standard deviation of experimental data. Clearly this figure shows as the *Kernel PDF* better fits experimental data.

The nominal displacement vector $\mathbf{u}_0^N$ is evaluated as follows :

$$\mathbf{u}_0^N = \mathbf{K}_0^{-1}\mathbf{F} \tag{41}$$

obtaining:

$$\mathbf{u}_0^N = \begin{pmatrix} u_{x1} \\ u_{y1} \\ u_{x2} \\ u_{y2} \end{pmatrix} = \begin{pmatrix} 4.29699 \\ 1.12239 \\ 5.41939 \\ 1.12239 \end{pmatrix} [\mathrm{mm}]; \tag{42}$$

To evaluate in explicit form the first two statistics of the response, the *Kernel PDF*, to satisfy the condition (13), has to be normalized into a lesser than 1 domain. This normalization has been performed by means of the following transformation:

$$\tilde{e} = \frac{\tilde{\alpha} - \mu_{\tilde{\alpha}}}{\mu_{\tilde{\alpha}}} \tag{43}$$

where $\mu_{\tilde{\alpha}}$ is the mean value of *Kernel PDF*. So operating the normalized *Kernel PDF* of uncertain elastic modulus, $p_E(\tilde{e})$, represented in Figure 3, lies into the interval domain $[-0.28, 0.28]$.

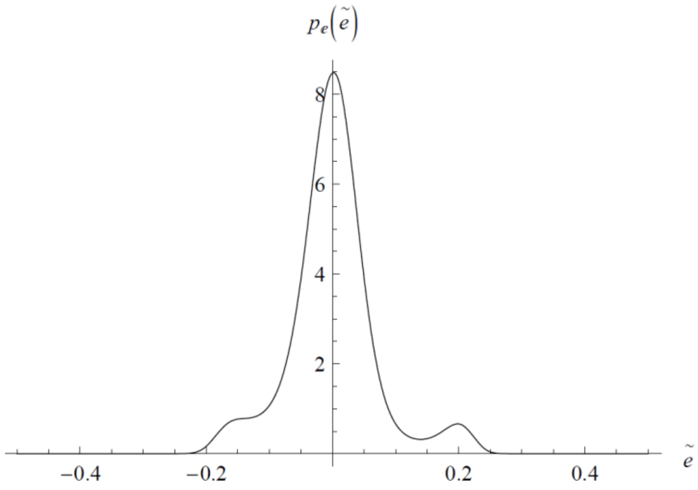

Figure 3. Normalized *Kernel PDF*.

To test the accuracy of proposed method, in Table II are reported the mean values, μ_{u_r} , and the standard deviations, σ_{u_r} , of displacements of studied structure, evaluated by means of Eqs. (17) and compared with the ones coming from *MCS*. In Table II the percentage errors are given, comparing the analytical data with the results obtained from *MCS* of 5000, 500 000, 1 000 000 samples. Negligible percentage errors confirm the accuracy of proposed method, provided a considerable reduction of the computational effort.

Table II. Comparison between stochastic results and Monte Carlo Simulation (Kernel Density).

Parameter [mm]	*analytical*	*MCS 5000*	*Error* [%]	*MCS 500000*	*Error* [%]	*MCS 10^6*	*Error* [%]
μ_{ux1}	4.31818	4.31884	0.0153	4.31854	0.0083	4.3180	-0.0037
μ_{uy1}	1.12793	1.12768	-0.0222	1.12796	0.0027	1.1280	0.0062
μ_{ux2}	5.44611	5.44564	-0.0086	5.44658	0.0086	5.4468	0.0127
μ_{uy2}	1.12793	1.12806	0.0115	1.12774	-0.0168	1.1280	0.0027
σ_{ux1}	0.23680	0.23715	0.1451	0.23677	-0.0114	0.2369	0.0355
σ_{uy1}	0.07893	0.07943	0.6288	0.07876	-0.2174	0.0789	-0.0390
σ_{ux2}	0.24961	0.25103	0.5669	0.24949	-0.0481	0.2496	0.0024
σ_{uy2}	0.07893	0.07801	-1.1898	0.07885	-0.1074	0.0789	0.0152

The same analytical approach has been applied assuming a *Gaussian PDF*. In Table III the percentage errors between analytical results and *MCS* with 1.000.000 samples are reported, confirming the accuracy of proposed method.

Table III. Comparison between stochastic results and Monte Carlo Simulation (Gaussian PDF).

Parameter[mm]	*analytical*	*MCS10*^{6}	*Error*[%]
μ_{ux1}	4.31834	4.31821	-0.0030
μ_{uy1}	1.12797	1.12807	0.0089
μ_{ux2}	5.44631	5.44601	-0.0055
μ_{uy2}	1.12797	1.12802	0.0044
σ_{ux1}	0.24032	0.240522	0.0856
σ_{uy1}	0.08011	0.0801257	0.0255
σ_{ux2}	0.25332	0.253463	0.0584
σ_{uy2}	0.08011	0.0801882	0.1034

Table IV summarizes the 3rd and 4th order central moments sorted by *MCS* using 10^6 samples, for the adopted densities.

Table IV. Comparison between 3rd and 4th order central momentsfor both PDF.

Parameter	*Kernel PDF*	*Gaussian PDF*
$\mu_{3,ux1}$ [mm^3]	0.0042728	0.0053643
$\mu_{3,uy1}$ [mm^3]	0.0001791	0.0002233
$\mu_{3,ux2}$ [mm^3]	0.0044510	0.0055959
$\mu_{3,uy2}$[mm^3]	0.0001784	0.0002263
$\mu_{4,ux1}$ [mm^4]	0.0138060	0.0111287
$\mu_{4,uy1}$ [mm^4]	0.0001831	0.0001398
$\mu_{4,ux2}$ [mm^4]	0.0160580	0.0134891
$\mu_{4,uy2}$[mm^4]	0.0001835	0.0001405

Such central moments combined with the *MCS* mean values and standard deviations are used to evaluate the *CoV*s, μ_u / σ_u, the skewness coefficients, $\mu_{3,u} / \sigma_u^3$, and excess kurtosis, $(\mu_{4,u} / \sigma_u^4) - 3$, of both *Kernel PDF* and *Gaussian PDF* in terms of displacements.

Due to nonlinear filtering of input data, it is well known that the expected structural response has property of non Gaussianity. Adopting the kernel density function, which takes in account of higher order statistics of the input data, the structural response statistics of order higher than the second gives results which are different from the ones sorted by simply assuming the Gaussianity of input data (i.e. taking into account the input data statistics up to the second order). Such consideration justifies the need to take into account of input data statistics of higher order to the second, when it is interesting to well catch the non Gaussian character of structural response.

On the other hand, the non Gaussianity of the response in both cases is highlighted by slightly right-tailed shape with respect to the mean of responses, as indicated by skewness coefficient, given in Table V where it is clearly evident that, adopting the *Kernel PDF*, the sensible higher value of excess kurtosis is provided.

Table V. C.O.V., skewness coefficients and excess kurtosis of the responses.

Parameter	*Kernel PDF*	*Gaussian PDF*
μ_{ux1}/σ_{ux1}	0.055	0.056
μ_{uy1}/σ_{u1}	0.070	0.071
μ_{ux2}/σ_{ux2}	0.046	0.047
μ_{uy2}/σ_{uy2}	0.070	0.071
$\mu_{3,ux1}/\sigma_{ux1}^3$	0.3214	0.3855
$\mu_{3,uy1}/\sigma^3{}_{uy1}$	0.3646	0.4342
$\mu_{3,ux2}/\sigma_{ux2}^3$	0.2862	0.3437
$\mu_{3,uy2}/\sigma_{uy2}^3$	0.3625	0.4390
$\frac{\mu_{4,ux1}}{\sigma^4{}_{ux1}}-3$	1.3845	0.3253
$\frac{\mu_{4,uy1}}{\sigma^4{}_{uy1}}-3$	1.7249	0.3909
$\frac{\mu_{4,ux2}}{\sigma^4{}_{ux2}}-3$	1.1361	0.2683
$\frac{\mu_{4,uy2}}{\sigma^4{}_{uy2}}-3$	1.7246	0.3985

4.2. INTERVAL ANALYSIS

It is well known that when the information on experimental data is incomplete or fragmentary, the interval analysis is a very efficient method to evaluate the propagation of the uncertainties on structural response. To define the interval of uncertainty, the knowledge of the distribution function is not required but its bounds only. Furthermore, according to the philosophy of interval analysis, the measured data define an interval with full confidence that the value is within the interval, and not outside it. That is, it is not a confidence interval or credibility interval. Rather, the interval represents sure bounds of the measurement, with full degree of confidence on experimental data (Ferson et al., 2007).

The starting point in using a bounded interval to model the measurement uncertainty is to acknowledge the intrinsic imprecision in measurement. In the studied truss structure, the population of experimental data is numerous, so that reliable results can be obtained by applying the probabilistic approach, described in the previous section. The aim of this section, is to compare the results provided by the probabilistic model with the ones evaluated by applying the *Improved Interval Analysis*. For this purpose, the first step is to define a reliable interval of the uncertain elastic modulus. A reasonable choice seems to be a normalized interval containing all experimental data, i.e. $[-0.28,+0.28]$, which has been chosen for Kernel PDF evaluation. In Table VI, the chosen values of *lower bound* (*LB*), $\underline{\alpha}$, and *upper bound* (*UB*), $\bar{\alpha}$, as well as the midpoint, $\mu_\alpha = (\bar{\alpha}+\underline{\alpha})/2$, deviation, $\Delta\alpha = (\bar{\alpha}-\underline{\alpha})/2$, and *Coefficient of Interval Uncertainty* (*C.I.U.*), $\Delta\alpha/\mu_\alpha$, are reported.

Table VI. Interval parameters for Young Elastic Modulus from experimental data (100% of experimental data).

$\underline{\alpha}$ [N/mm^2]	142638.10
$\bar{\alpha}$ [N/mm^2]	253583.26
μ_α [N/mm^2]	198110.68
$\Delta\alpha$ [N/mm^2]	110945.16
$C.I.U.$	0.28

The corresponding midpoint displacement vector $\mathbf{u}_0$ and the lower and the upper bounds of displacements vectors calculated by Eqs. (30) and (31) are given respectively as:

$$\mathbf{u}_0 = \begin{pmatrix} 4.66256 \\ 1.21788 \\ 5.88044 \\ 1.21788 \end{pmatrix} [\mathrm{mm}] \quad \underline{\mathbf{u}} = \begin{pmatrix} 3.35701 \\ 0.87686 \\ 4.23387 \\ 0.87686 \end{pmatrix} [\mathrm{mm}]; \quad \bar{\mathbf{u}} = \begin{pmatrix} 5.96811 \\ 1.55890 \\ 7.52701 \\ 1.55890 \end{pmatrix} [\mathrm{mm}];$$

The difference between midpoint values and explicit mean value vectors for *Kernel PDF* and *Gaussian PDF*, reported in Table II and Table III, is reported in Table VII.

In Figures 4-7 the bounds of interval responses, in terms of displacement, sorted by *Improved Interval Analysis*, are compared with the results obtained in terms of confidence range displacements, calculated as the mean value ± three times standard deviation of stochastic results, coming out by assuming maximum entropy approach and adopting the normal distribution. These Figures show that for the analysed truss structure, the confidence range lie into the bounds defined by *Interval Analysis*, if an interval that includes all experimental data is chosen.

Table VII. Comparison between mean values and midpoint displacements.

Parameter [mm]	$\mathbf{u}_0$	$\boldsymbol{\mu}_{\tilde{U}}$ *(Kernel PDF)*	$\boldsymbol{\mu}_{\tilde{U}}$ *(Gaussian PDF)*	*Difference* [%] *(Kernel PDF)*	*Difference* [%] *(Gaussian PDF)*
μ_{ux1}	4.66256	4.31818	4.31834	7.3861	7.3826
μ_{uy1}	1.21788	1.12793	1.12797	7.3858	7.3825
μ_{ux2}	5.88044	5.44611	5.44631	7.3860	7.3826
μ_{uy2}	1.21788	1.12793	1.12797	7.3858	7.3825

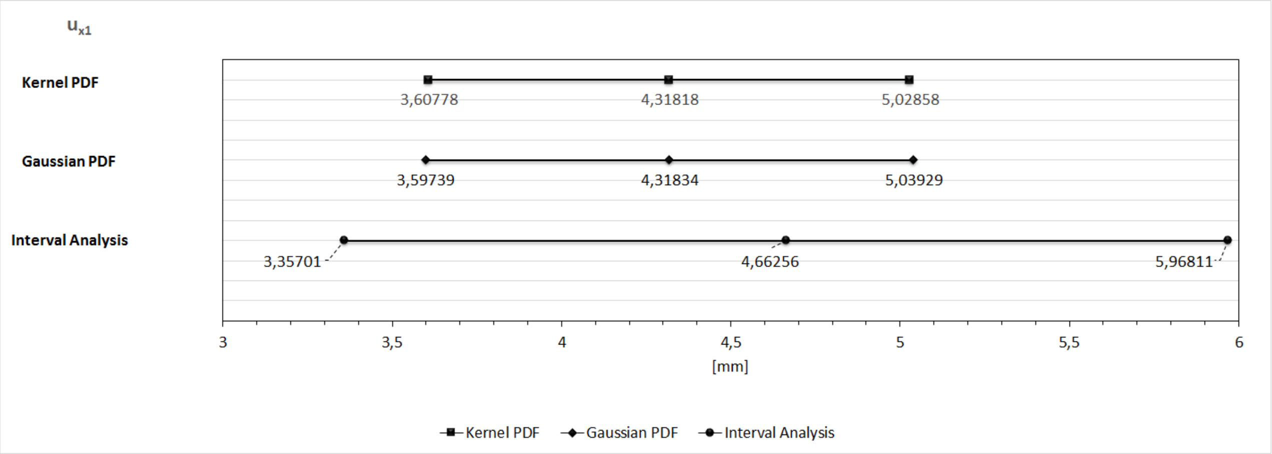

Figure 4. u_{x1}: interval analysis bounds and *Kernel* and *Gaussian PDF* $\mu_u \pm 3\sigma_u$.

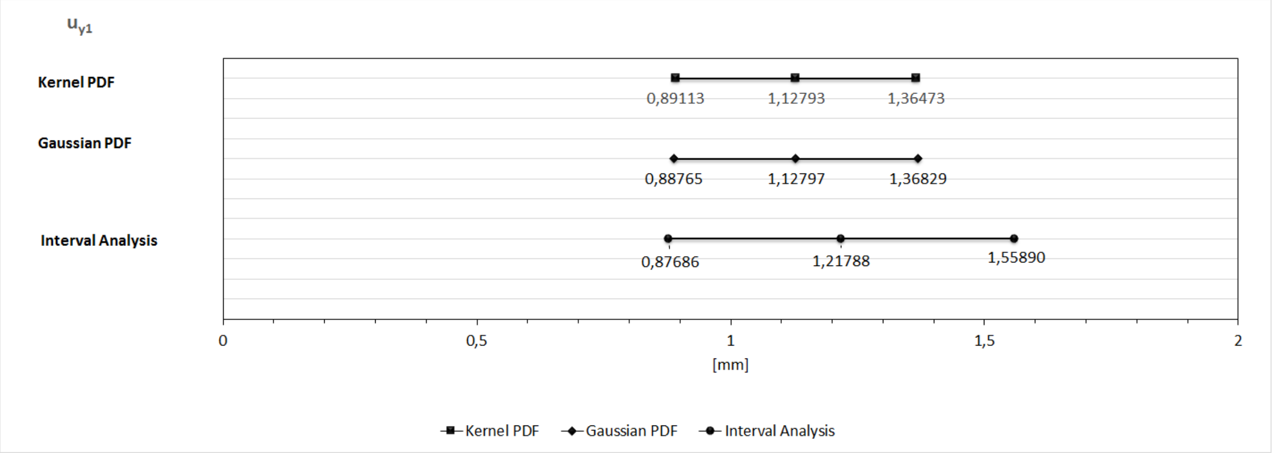

Figure 5. u_{y1}: interval analysis bounds and *Kernel* and *Gaussian PDF* $\mu_u \pm 3\sigma_u$.

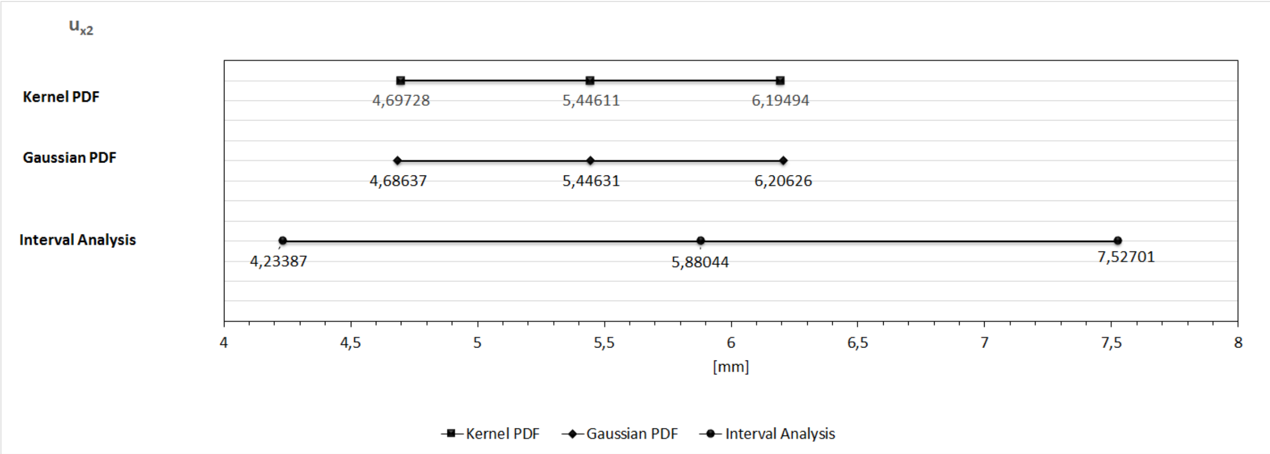

Figure 6. u_{x2}: interval analysis bounds and *Kernel* and *Gaussian PDF* $\mu_u \pm 3\sigma_u$.

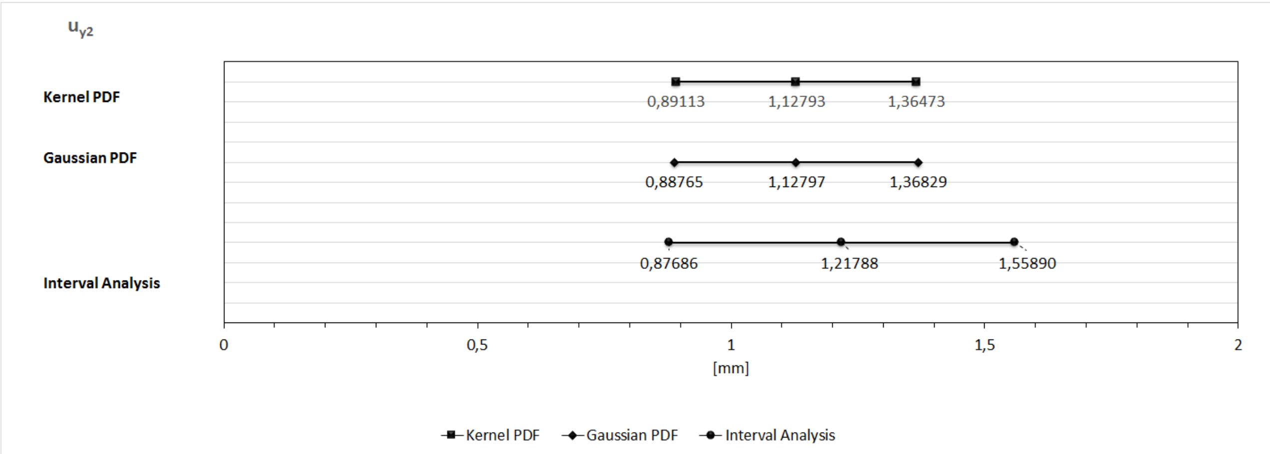

Figure 7. u_{y2}: interval analysis bounds and *Kernel* and *Gaussian PDF* $\mu_u \pm 3\sigma_u$.

5. Conclusions

Starting from tensile tests performed on steel bars, where elastic moduli are measured, the PDF of uncertain elastic modulus was recovered by maximum entropy approach. This function was adopted for the static analysis of a truss structure to evaluate stochastic structural response by means the *Rational Series Expansion* technique. The comparison with Monte Carlo Simulation results confirmed the accuracy of method.

In order to compare the results provided by the probabilistic model with the ones evaluated by applying the *Improved Interval Analysis*, the confidence range displacement, calculated as the mean value ± three times standard deviation of stochastic results, is determined. Then the bounds of the response interval by applying the *Improved Interval Analysis* are evaluated. The comparison of two response intervals showed that the selected confidence range lies into the bounds defined by Interval Analysis if, for the uncertain elastic modulus, the interval that includes all experimental data is chosen.

References

Alibrandi U. and G. Ricciardi. Efficient evaluation of the pdf of a random variable through the kernel density maximum entropy approach. *International Journal for Numerical Methods in Engineering*, 75:1511–1548, 2008.

Barbato G., E. M. Barini, G. Genta and R. Levi. Features and performance of some outlier detection methods. *Journal of Applied Statistics*, 38:2133–2149, 2011.

Elishakoff I. and M. Ohsaki. Optimization and Anti-optimization of Structures under Uncertainty, Imperial College Press, London, 2010.

Ferson S., V. Kreinovich, J. Hajagos, W. Oberkampf and L. Ginzburg. *Experimental Uncertainty Estimation and Statistics for Data Having Interval Uncertainty*. SANDIA REPORT: SAND 2007-0939, 2007.

Moens, D. and D. Vandepitte. A Survey of Non-Probabilistic Uncertainty Treatment in Finite Element Analysis. *Computer Methods in Applied Mechanics and Engineering* 194:1527–1555, 2005.

Moore, R. E. *Interval Analysis*, Prentice-Hall, Englewood Cliffs, 1966.

Moore, R. E., R. B. Kearfott and M. J. Cloud. *Introduction to Interval Analysis*, SIAM, Philadelphia, USA, 2009.

Muhanna, R. L. and R. L. Mullen. Uncertainty in Mechanics: Problems-Interval-Based Approach. *Journal Engineering Mechanics ASCE* 127:557-566, 2001.

Muscolino G. and A. Sofi. Stochastic Analysis of Structures with Uncertain-but-Bounded Parameters via Improved Interval Analysis. *Probabilistic Engineering Mechanics* 28:152-163, 2012.

Muscolino, G. and A. Sofi. Bounds for the Stationary Stochastic Response of Truss Structures with Uncertain-but-Bounded Parameters. *Mechanical Systems and Signal Processing* 37:163-181, 2013.

Muscolino G., R. Santoro and A. Sofi. Explicit frequency response functions of discretized structures with uncertain parameters. *Computer and Structures*, 133:64-78, 2014.